Polarizations of χ_{c1} and χ_{c2} in Prompt Production at the LHC

Hua-Sheng Shao,[1] Yan-Qing Ma,[2] Kai Wang,[1] and Kuang-Ta Chao[1,3,4]

[1]School of Physics and State Key Laboratory of Nuclear Physics and Technology, Peking University, Beijing 100871, China

[2]Physics Department, Brookhaven National Laboratory, Upton, New York 11973, USA

[3]Collaborative Innovation Center of Quantum Matter, Beijing 100871, China

[4]Center for High Energy Physics, Peking University, Beijing 100871, China

(Received 13 February 2014; published 8 May 2014)

Prompt χ_c production at hadron colliders may provide a unique test for the color-octet mechanism in nonrelativistic QCD. We present an analysis for the polarization observables of χ_{c1} and χ_{c2} at next-to-leading order in α_S and propose to measure them at the LHC, which is expected to be important for testing the validity of nonrelativistic QCD.

DOI: 10.1103/PhysRevLett.112.182003 PACS numbers: 12.38.Bx, 13.60.Le, 13.88.+e, 14.40.Pq

Heavy quarkonium production provides an ideal laboratory to understand quantum chromodynamics. In contrast to the helicity-summed cross section, the quarkonium polarization measurement may provide more complete information for the production mechanism of heavy quarkonium [1].

A distinct example is the J/ψ polarization at hadron colliders. The polar asymmetry coefficient λ_θ in the angular distribution of the leptons from the J/ψ decay is an important observable that encodes the J/ψ polarization information. At the Tevatron, the CDF Collaboration measured the quantity many years ago [2,3]. Their measurements show that λ_θ for prompt J/ψ production in its helicity frame is around zero up to $p_T = 30$ GeV, indicating that the J/ψ mesons are produced in the unpolarized pattern. The state-of-the-art theory that describes the heavy quarkonium dynamics, nonrelativistic QCD (NRQCD) [4], predicts that the heavy quark pair is allowed to be created in a color-octet (CO) intermediate state at short distances and then evolves nonperturbatively into a color-singlet (CS) quarkonium at long distances. Although this CO mechanism provides an opportunity to account for the CDF yield data [5,6] that cannot be resolved in the CS model (CSM) even by including the higher-order QCD corrections [7,8], the leading-order (LO) in α_S NRQCD prediction gives a completely transverse polarization result at high p_T due to gluon fragmentation to the CO ${}^3S_1^{[8]}$ intermediate state [9]. Recently, three groups reported their next-to-leading order (NLO) QCD corrections to the J/ψ polarization [10–12]. Recall that the J/ψ polarization is strongly dependent on the specific choice of the nonperturbative long-distance matrix elements (LDMEs), which can only be determined from the experimental data. Choosing different p_T regions of the input experimental data may result in very different predictions. Therefore, the precise measurement of polarization, especially at high p_T, may provide a smoking-gun signature to distinguish between various production mechanisms of heavy quarkonium. Moreover, it was pointed out in Ref. [11] that there is still a CO LDMEs parameter space left to make both the helicity-summed yields and λ_θ quite satisfactory compared to the hadroproduction data.

However, the prompt J/ψ production at the Tevatron and LHC is affected substantially by the higher charmonia (e.g., χ_c and ψ') transitions to J/ψ. Furthermore, even for direct J/ψ production, there are three leading CO LDMEs, which makes the precise determination of CO LDMEs difficult. In contrast, for the χ_c hadroproduction the feed-down contribution only comes from ψ' to χ_c transitions, but they are not insignificant, and there is only one leading CO state ${}^3S_1^{[8]}$ involving χ_c direct production, which can make the determination of the LDMEs easier and more precise. Moreover, the higher-order QCD corrections to the conventional P-wave CS state suffer from severe infrared divergences, whereas in NRQCD these divergences can be absorbed by the CO state and, thus, make the P-wave observables well defined beyond LO. Given these reasons, the investigation of χ_c production at the LHC is an important way to test the validity of NRQCD factorization and the CO mechanism.

The first investigation for the helicity-summed χ_c hadroproduction at NLO level was performed in Ref. [13]. In this Letter, we extend our calculation to the polarized case, with the method described in Refs. [11,14]. The polarization observables of χ_{c1} and χ_{c2} were proposed in Refs. [15–17]. Experimentally, one may have two ways to measure the polarization of χ_{c1} and χ_{c2} through the angular distributions of their decay products. One is to measure the J/ψ angular distribution from $\chi_c \to J/\psi\gamma$. The angular distribution with respect to the J/ψ polar angle θ in the rest frame of χ_c can be formulated as [17]

$$\frac{d\mathcal{N}^{\chi_{cJ}}}{d\cos\theta} \propto 1 + \sum_{k=1}^{J} \lambda_{k\theta}\cos^{2k}\theta, \qquad (1)$$

where the polar asymmetry coefficients $\lambda_{k\theta}$ can be expressed as the rational functions of the χ_{cJ} production spin density matrix $\rho^{\chi_{cJ}}$. More specifically, for χ_{c1} it is

$$\lambda_\theta = (1-3\delta)\frac{N_{\chi_{c1}} - 3\rho_{0,0}^{\chi_{c1}}}{(1+\delta)N_{\chi_{c1}} + (1-3\delta)\rho_{0,0}^{\chi_{c1}}}, \quad (2)$$

with $N_{\chi_{c1}} \equiv \rho_{1,1}^{\chi_{c1}} + \rho_{0,0}^{\chi_{c1}} + \rho_{-1,-1}^{\chi_{c1}}$, whereas for χ_{c2}, the coefficients are

$$\lambda_\theta = 6[(1-3\delta_0-\delta_1)N_{\chi_{c2}} - (1-7\delta_0+\delta_1)(\rho_{1,1}^{\chi_{c2}} + \rho_{-1,-1}^{\chi_{c2}}) - (3-\delta_0-7\delta_1)\rho_{0,0}^{\chi_{c2}}]/R,$$
$$\lambda_{2\theta} = (1+5\delta_0-5\delta_1)[N_{\chi_{c2}} - 5(\rho_{1,1}^{\chi_{c2}} + \rho_{-1,-1}^{\chi_{c2}}) + 5\rho_{0,0}^{\chi_{c2}}]/R, \quad (3)$$

with

$$N_{\chi_{c2}} = \rho_{2,2}^{\chi_{c2}} + \rho_{1,1}^{\chi_{c2}} + \rho_{0,0}^{\chi_{c2}} + \rho_{-1,-1}^{\chi_{c2}} + \rho_{-2,-2}^{\chi_{c2}},$$
$$R = (1+5\delta_0+3\delta_1)N_{\chi_{c2}} + 3(1-3\delta_0-\delta_1)(\rho_{1,1}^{\chi_{c2}} + \rho_{-1,-1}^{\chi_{c2}}) + (5-7\delta_0-9\delta_1)\rho_{0,0}^{\chi_{c2}}.$$

The parameters δ, δ_0, and δ_1 can be determined by the normalized multipole amplitudes. Following the notations in Ref. [18], we denote the normalized electric dipole ($E1$) transition amplitudes by $a_1^{J=1}$ and $a_1^{J=2}$ for χ_{c1} and χ_{c2}, respectively, while $a_2^{J=1}, a_2^{J=2}, a_3^{J=2}$ are the χ_{c1} and χ_{c2} normalized magnetic quadrupole ($M2$) amplitudes and χ_{c2} electric octupole amplitude ($E3$). We remind readers that the word "normalized" here means we have relations $a_1^{J=1} + a_2^{J=1} = 1$ and $a_1^{J=2} + a_2^{J=2} + a_3^{J=2} = 1$. The explicit expressions for $\delta, \delta_0, \delta_1$ are

$$\delta = (1 + 2a_1^{J=1}a_2^{J=1})/2,$$
$$\delta_0 = [1 + 2a_1^{J=2}(\sqrt{5}a_2^{J=2} + 2a_3^{J=2}) + 4a_2^{J=2}(a_2^{J=2} + \sqrt{5}a_3^{J=2}) + 3(a_3^{J=2})^2]/10,$$
$$\delta_1 = [9 + 6a_1^{J=2}(\sqrt{5}a_2^{J=2} - 4a_3^{J=2}) - 4a_2^{J=2}(a_2^{J=2} + 2\sqrt{5}a_3^{J=2}) + 7(a_3^{J=2})^2]/30. \quad (4)$$

An alternative way to study the polarizations of χ_{c1} and χ_{c2} is to measure the dilepton angular distributions from $\chi_{cJ} \to J/\psi\gamma \to l^+l^-\gamma$. There are two choices to describe the dilepton angular distributions [16,17]. Here, we only choose the second one presented in Ref. [17], where the z axis in the rest frame of J/ψ coincides with the direction of the spin quantization axis in the χ_c rest frame. The generic lepton polar angle θ' dependence is

$$\frac{d\mathcal{N}^{\chi_{cJ}}}{d\cos\theta'} \propto 1 + \lambda_{\theta'}\cos^2\theta', \quad (5)$$

where

$$\lambda_{\theta'}^{\chi_{c1}} = \frac{-N_{\chi_{c1}} + 3\rho_{0,0}^{\chi_{c1}}}{R_1},$$
$$\lambda_{\theta'}^{\chi_{c2}} = \frac{6N_{\chi_{c2}} - 9(\rho_{1,1}^{\chi_{c2}} + \rho_{-1,-1}^{\chi_{c2}}) - 12\rho_{0,0}^{\chi_{c2}}}{R_2}, \quad (6)$$

with

$$R_1 = [(15 - 2(a_2^{J=1})^2)N_{\chi_{c1}} - (5 - 6(a_2^{J=1})^2)\rho_{0,0}^{\chi_{c1}}]/(5 - 6(a_2^{J=1})^2),$$
$$R_2 = [2(21 + 14(a_2^{J=2})^2 + 5(a_3^{J=2})^2)N_{\chi_{c2}} + 3(7 - 14(a_2^{J=2})^2 - 5(a_3^{J=2})^2)(\rho_{1,1}^{\chi_{c2}} + \rho_{-1,-1}^{\chi_{c2}}) + 4(7 - 14(a_2^{J=2})^2 - 5(a_3^{J=2})^2)\rho_{0,0}^{\chi_{c2}}] \div [7 - 14(a_2^{J=2})^2 - 5(a_3^{J=2})^2].$$

Note that $\lambda_{2\theta}$ for χ_{c2} is suppressed by the higher-order multipole amplitudes $a_2^{J=2}, a_3^{J=2}$. The observable is expected to be near zero. Hence, we refrain from establishing the p_T distribution of $\lambda_{2\theta}$ here.

In our numerical computation, we choose the same input parameters as those presented in Ref. [11]. The renormalization scale μ_r, factorization scales μ_f, and NRQCD scale μ_Λ are chosen as $\mu_r = \mu_f = \sqrt{4m_c^2 + p_T^2}$ and $\mu_\Lambda = m_c$. The CO LDMEs are chosen to be $\langle\mathcal{O}^{\chi_{cJ}}(^3S_1^{[8]})\rangle = (2J+1)\times(2.2^{+0.48}_{-0.32})\times 10^{-3}\,\mathrm{GeV}^3$ [13], which are obtained by fitting

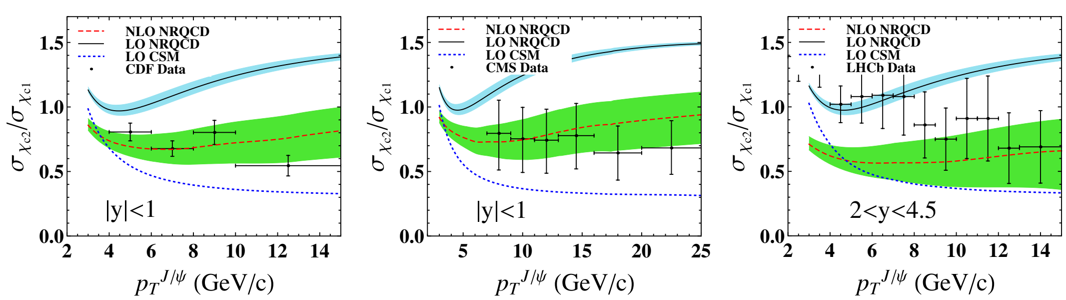

FIG. 1 (color online). The cross section ratio $\sigma_{\chi_{c2}}/\sigma_{\chi_{c1}}$ vs the transverse momentum $p_T^{J/\psi}$ at the Tevatron Run II (left panel) and LHC at $\sqrt{S} = 7$ TeV (right two panels). The rapidity cuts are the same as in the experiments [19,23,24]. Results for LO NRQCD (solid lines), NLO NRQCD (dashed lines), and LO CSM (dotted lines) are shown.

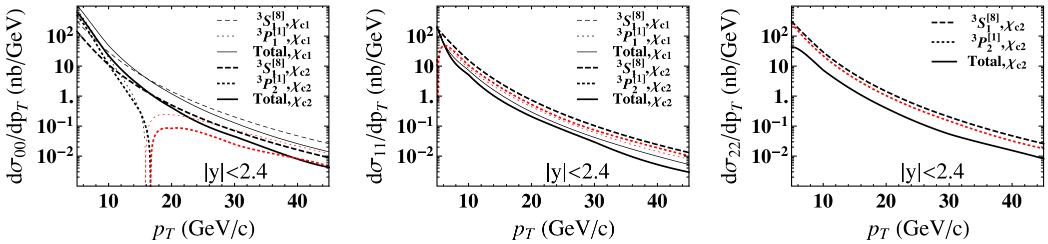

FIG. 2 (color online). $d\sigma_{00}/dp_T$, $d\sigma_{11}/dp_T$, $d\sigma_{22}/dp_T$ for $pp \to \chi_{cJ} + X(J = 1, 2)$ with $\sqrt{S} = 7$ TeV and $|y| < 2.4$ in the helicity frame at NLO in NRQCD. The thin lines represent χ_{c1} whereas the thick lines represent χ_{c2}. Negative values are marked red (lighter).

the ratio $\sigma_{\chi_{c2}}/\sigma_{\chi_{c1}}$ at NLO level to the CDF data [19], while the CS LDMEs are estimated using the B-T potential model [20] as $\langle\mathcal{O}(^3S_J^{[1]})\rangle = (2J+1)[(3|R'(0)|^2)/4\pi]$ with $|R'(0)|^2 = 0.075$ GeV^5. The uncertainties due to the scale dependence, which is estimated by varying μ_r, μ_f by a factor of $\frac{1}{2}$ to 2 with respect to their central values, the charm quark mass $m_c = 1.5 \pm 0.1$ GeV, and the error in the CDF data [19] are all encoded in the error estimations of the CO LDMEs. The normalized multipole amplitudes used here are taken from the CLEO measurement [18], i.e., $a_2^{J=1} = (-6.26 \pm 0.68) \times 10^{-2}, a_2^{J=2} = (-9.3 \pm 1.6) \times 10^{-2}, a_3^{J=2} = 0$. We keep the $E3$ amplitude $a_3^{J=2}$ vanishing, which is the consequence of the single quark radiation hypothesis [21,22].

As was done in Ref. [13], we have tried to improve the uncertainties in the ratio $r \equiv m_c^2\langle\mathcal{O}^{\chi_{c0}}(^3S_1^{[8]})\rangle/\langle\mathcal{O}^{\chi_{c0}}(^3S_0^{[1]})\rangle$ by using the LHCb data [23] and CMS data [24]. With the Tevatron data, it was determined to be $r = 0.27 \pm 0.06$. But its accuracy is not improved significantly with the updated LHC data. With the LHCb data [23], r varies from 0.35 to 0.31 when using a different p_T cutoff. (To be compatible with our J/ψ case [11], we always ignore the data when $p_T < 7$ GeV.) Using the CMS data [24], we find r has very weak dependence on p_T cutoff, and its value is almost 0.25 with unpolarized hypothesis. The substantial uncertainty in the r extraction is due to different polarization hypotheses. The r value changes from 0.21 to 0.31 in two extreme hypotheses [24]. Here, we may choose $r = 0.27 \pm 0.06$ as an acceptable value, and the values of r from different extractions are well embodied in its uncertainties. We emphasize further that measurements with higher resolution, especially in the high p_T region, will be very useful to improve our NRQCD predictions.

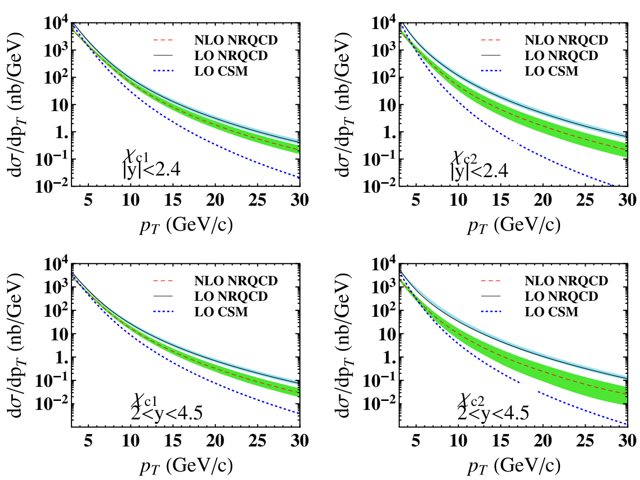

FIG. 3 (color online). Predictions of p_T spectra for the helicity-summed χ_{c1} (left column) and χ_{c2} (right column) at the LHC with $\sqrt{S} = 7$ TeV. Cross sections in the central rapidity region ($|y| < 2.4$) and forward rapidity region ($2 < y < 4.5$) for χ_c are plotted. Results for LO NRQCD (solid lines), NLO NRQCD (dashed lines), and LO CSM (dotted lines) are shown.

In Fig. 1, the cross section ratios $\sigma_{\chi_{c2}}/\sigma_{\chi_{c1}}$ at the Tevatron Run II and LHC are shown. For comparison, besides the NLO NRQCD predictions, we also plot the LO NRQCD results and the LO CSM results. We see that the NLO NRQCD results are consistent with the CDF data [19] and the CMS data [24] in the whole $p_T^{J/\psi}$ region, while in the forward rapidity region the NLO NRQCD prediction is in agreement with the LHCb data [23] only when $p_T^{J/\psi} > 8$ GeV, which may imply that some unknown nonperturbative effects make our fixed-order results unreliable when $p_T^{J/\psi}$ is lower. Note that $p_T^{J/\psi}$ is obtained from p_T of χ_c by the mass rescaling $p_T^{J/\psi} = m_{J/\psi}/m_{\chi_{cJ}} p_T$, which is proven to be a good approximation by the Monte Carlo simulation. Here, the masses $m_{J/\psi} = 3.10$ GeV, $m_{\chi_{c1}} = 3.51$ GeV, $m_{\chi_{c2}} = 3.56$ GeV, and branching ratios $\text{Br}(\chi_{c1} \to J/\psi\gamma) = 0.344, \text{Br}(\chi_{c2} \to J/\psi\gamma) = 0.195$ are taken from Ref. [25]. We see also that the LO CSM prediction is substantially lower than the experimental data. Two other important obstacles for CSM are the measured cross section of χ_{cJ} at the Tevatron Run I [13] and ratio $\sigma(\chi_{cJ} \to J/\psi\gamma)/\sigma(J/\psi)$ at the LHC [26]. While there are discrepancies between the LO CSM predictions and the

TABLE I. Upper and lower bound values of the observables λ_θ and $\lambda_{\theta'}$ for χ_{c1} and χ_{c2}.

Observable	$\lambda_\theta^{\chi_{c1}}$	$\lambda_\theta^{\chi_{c2}}$	$\lambda_{\theta'}^{\chi_{c1}}$	$\lambda_{\theta'}^{\chi_{c2}}$
Upper bound	0.556	1.61	0.994	0.928
Lower bound	−0.217	−0.803	−0.332	−0.574

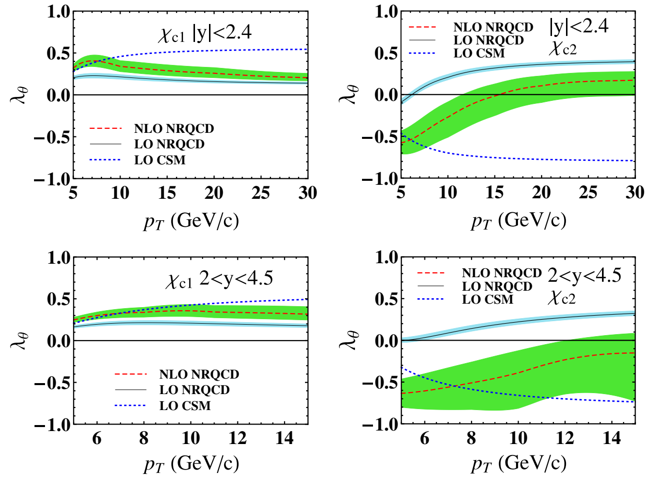

FIG. 4 (color online). The p_T dependence of λ_θ with J/ψ angular distributions from radiative decays $\chi_{c1} \to J/\psi\gamma$ (left column) and $\chi_{c2} \to J/\psi\gamma$ (right column) in the helicity frame at the LHC with $\sqrt{S} = 7$ TeV. Results in central and forward rapidity regions are plotted. The LO NRQCD (solid lines), NLO NRQCD (dashed lines), and LO CSM (dotted lines) predictions are shown.

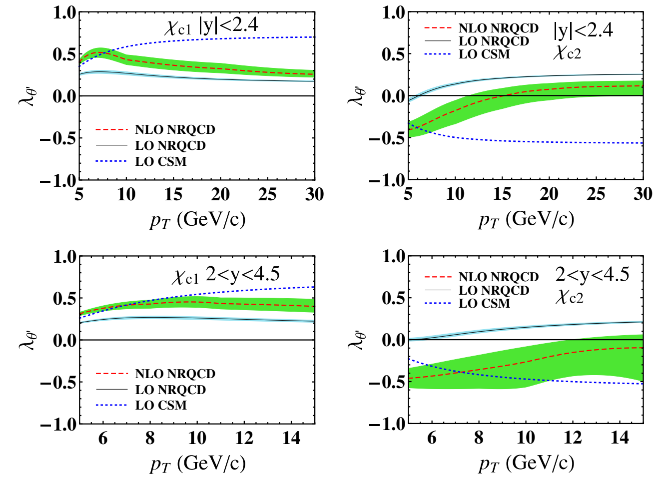

FIG. 5 (color online). The p_T dependence of $\lambda_{\theta'}$ with dilepton angular distributions from cascade decays $\chi_{c1} \to J/\psi\gamma \to l^+l^-\gamma$ (left column) and $\chi_{c2} \to J/\psi\gamma \to l^+l^-\gamma$ (right column) in the helicity frame at the LHC with $\sqrt{S} = 7$ TeV. Results in central rapidity and forward rapidity regions are plotted, and the LO NRQCD (solid lines), NLO NRQCD (dashed lines), and LO CSM (dotted lines) predictions are shown.

experimental data, the NLO NRQCD results are reasonably good. To present the predictions of the cross sections at the LHC, we also show the corresponding curves in Fig. 3. In Fig. 2, we present the curves of spin density matrix elements $d\sigma_{00}/dp_T, d\sigma_{11}/dp_T$ (and $d\sigma_{22}/dp_T$) for $\chi_{c1}(\chi_{c2})$ with $\sqrt{S} = 7$ TeV and $|y| < 2.4$. To be more specific, we also show curves in different Fock states (with LDMEs given above). The negative values (see also Refs. [10–13]) are marked red.

For the numerical results of the polarization observables of χ_{c1} and χ_{c2}, we use expressions in Eqs. (2), (3), and (6) and obtain, first, the lower and upper bound values of λ_θ and $\lambda_{\theta'}$ for χ_c regardless of its production mechanisms. They are presented in Table I. When $\rho^{\chi_{c1}}_{1,1} = \rho^{\chi_{c1}}_{-1,-1} \ll \rho^{\chi_{c1}}_{0,0}$, the polar observables for χ_{c1} approach their maximal values, whereas the minimal values are obtained when $\rho^{\chi_{c1}}_{1,1} = \rho^{\chi_{c1}}_{-1,-1} \gg \rho^{\chi_{c1}}_{0,0}$. For χ_{c2}, the polar asymmetry coefficients λ_θ and $\lambda_{\theta'}$ are maximum when $\rho^{\chi_{c2}}_{2,2} = \rho^{\chi_{c1}}_{-2,-2} \gg \rho^{\chi_{c2}}_{1,1} = \rho^{\chi_{c2}}_{-1,-1}, \rho^{\chi_{c2}}_{0,0}$ and minimum when $\rho^{\chi_{c2}}_{2,2} = \rho^{\chi_{c1}}_{-2,-2}, \rho^{\chi_{c2}}_{1,1} = \rho^{\chi_{c2}}_{-1,-1} \ll \rho^{\chi_{c2}}_{0,0}$. The p_T distributions of λ_θ and $\lambda_{\theta'}$ are shown in Figs. 4 and 5, respectively. It is worth noting that the transformation relation between the spin density matrices of ${}^3S_1^{[8]}$ and those of ${}^3S_J^{[1]}$ [17]

$$\rho^{{}^3S_1^{[8]} \to \chi_{cJ}}_{J_z,J'_z} \propto \sum_{l_z,s_z,s'_z=\pm 1,0} \rho^{{}^3S_1^{[8]}}_{s_z,s'_z} \times \langle 1, l_z; 1, s_z | J, J_z \rangle \langle 1, l_z; 1, s'_z | J, J'_z \rangle \quad (7)$$

is used in our numerical results. The error bands in these figures are due to uncertainties of the CO LDMEs $\langle \mathcal{O}^{\chi_{cJ}}({}^3S_1^{[8]}) \rangle$ and errors in the normalized multipole amplitudes. From Figs. 4 and 5, we see that the measurements of these polarization observables may provide another important way to test the CO mechanism in the hadroproduction of heavy quarkonium.

In summary, we have performed an analysis of the polarized χ_{c1} and χ_{c2} production at the LHC in NRQCD and in the color-singlet model. The complete NLO NRQCD predictions are given for the first time. These observables may provide important information, which is not available in the helicity-summed p_T spectra, in testing the validity of NRQCD factorization. Compared with J/ψ production, the prompt χ_c production may play a unique role in understanding the heavy quarkonium production mechanism. Therefore, we propose to measure these polarization observables at the LHC.

We are grateful to C. Meng, Y. J. Zhang, and H. Han for helpful discussions. This work was supported in part by the National Natural Science Foundation of China (No. 11021092 and No. 11075002). Y.-Q. M is supported by the U.S. Department of Energy, Contract No. DE-AC02-98CH10886.

[1] N. Brambilla *et al.*, Eur. Phys. J. C **71**, 1534 (2011).
[2] T. Affolder *et al.* (CDF Collaboration), Phys. Rev. Lett. **85**, 2886 (2000).
[3] A. Abulencia *et al.* (CDF Collaboration), Phys. Rev. Lett. **99**, 132001 (2007).
[4] G. T. Bodwin, E. Braaten, and G. P. Lepage, Phys. Rev. D **51**, 1125 (1995).

[5] F. Abe *et al.* (CDF Collaboration), Phys. Rev. Lett. **79**, 572 (1997).
[6] F. Abe *et al.* (CDF Collaboration), Phys. Rev. Lett. **79**, 578 (1997).
[7] J. M. Campbell, F. Maltoni, and F. Tramontano, Phys. Rev. Lett. **98**, 252002 (2007).
[8] J. Lansberg, Eur. Phys. J. C **61**, 693 (2009).
[9] E. Braaten, B. A. Kniehl, and J. Lee, Phys. Rev. D **62**, 094005 (2000).
[10] M. Butenschoen and B. A. Kniehl, Phys. Rev. Lett. **108**, 172002 (2012).
[11] K.-T. Chao, Y.-Q. Ma, H.-S. Shao, K. Wang, and Y.-J. Zhang, Phys. Rev. Lett. **108**, 242004 (2012).
[12] B. Gong, L.-P. Wan, J.-X. Wang, and H.-F. Zhang, Phys. Rev. Lett. **110**, 042002 (2013).
[13] Y.-Q. Ma, K. Wang, and K.-T. Chao, Phys. Rev. D **83**, 111503 (2011).
[14] H.-S. Shao, Comput. Phys. Commun. **184**, 2562 (2013).
[15] B. A. Kniehl, G. Kramer, and C. P. Palisoc, Phys. Rev. D **68**, 114002 (2003).
[16] P. Faccioli, C. Lourenco, J. Seixas, and H. K. Wohri, Phys. Rev. D **83**, 096001 (2011).
[17] H.-S. Shao and K.-T. Chao, arXiv:1209.4610.
[18] M. Artuso *et al.* (CLEO Collaboration), Phys. Rev. D **80**, 112003 (2009).
[19] A. Abulencia *et al.* (CDF Collaboration), Phys. Rev. Lett. **98**, 232001 (2007).
[20] E. J. Eichten and C. Quigg, Phys. Rev. D **52**, 1726 (1995).
[21] G. Karl, S. Meshkov, and J. L. Rosner, Phys. Rev. Lett. **45**, 215 (1980).
[22] M. G. Olsson, C. J. Suchyta, A. D. Martin, and W. J. Stirling, Phys. Rev. D **31**, 1759 (1985).
[23] R. Aaij *et al.* (LHCb Collaboration), Phys. Lett. B **714**, 215 (2012).
[24] S. Chatrchyan *et al.* (CMS Collaboration), Eur. Phys. J. C **72**, 2251 (2012).
[25] K. Nakamura (Particle Data Group), J. Phys. G **37**, 075021 (2010).
[26] R. Aaij *et al.* (LHCb Collaboration), Phys. Lett. B **718**, 431 (2012).